CHAPTER 12

The Use of Gelatin Substrates for Traction Force Microscopy in Rapidly Moving Cells

Juliet Lee

Department of Molecular and Cell Biology
University of Connecticut
Storrs, Connecticut 06269

The study of traction forces generated by rapidly moving cells requires the use of substrates that are highly elastic because these cells typically generate weaker traction forces than slower moving cells. Gelatin substrates are soft enough to allow deformation by rapidly moving cells such as fish epidermal keratocytes and *Dictyostelium discoideum* amoebas. In addition, gelatin substrates are thin ($\sim$30–40 μm) and transparent, allowing them to be used in combination with high-resolution calcium imaging. Importantly, the responsiveness of gelatin substrates allows changes in traction force generation to be detected within seconds, corresponding to the timescale of calcium transients. Here we describe the manufacture and application of gelatin substrates to study the role of mechanochemical signaling in the regulation of keratocyte movement. We show how patterns of

0091-679X/07 $35.00
DOI: 10.1016/S0091-679X(07)83012-3

traction force generation can be analyzed from a time series of traction vector maps, and how to interpret them in relation to cell movement. In addition, we discuss how the gelatin traction force assay is being used to study the mechanics of *Dictyostelium* cell motility, and future applications such as the study of neuronal path finding.

I. Introduction

Cells can respond to a wide range of mechanical stimuli such as fluid flow (Malek and Izumo, 1996), mechanical stretching (Pender and McCullouch, 1991), and even their own area of spreading (Chen *et al*., 1997). In addition, cells can respond to physical properties of their microenvironment (Chicurel *et al*., 1998; Janmey, 1998). For example, moving cells can sense the rigidity of their substrate (Lo *et al*., 2000), surface topology (Dunn and Brown, 1986), and changes in cytoskeletal tension (Lee *et al*., 1999). Au1

Cell movement requires the generation of mechanical forces (Lauffenburger and Horwitz, 1996; Schwarzbauer, 1997) including a protrusive force at the front cell edge, together with contractile forces to shift the cell body forward and to facilitate retraction at the rear. In addition, the strength of adhesion between cell and its substrate must be regulated so that newly formed adhesions at the cell front strengthen, while older ones at the rear disassemble (Sheetz *et al*., 1998). Although much is known about the molecular basis of various subprocesses of cell migration, such as protrusion, retraction, contractile force generation, and adhesion, we still do not understand how these processes are coordinated spatially or temporally. The generation of mechanical force is believed to play a central role in integrating different molecular processes to produce movement at the cellular level (Lauffenburger and Horwitz, 1996; Wang and Ingber, 1994).

The first study of traction forces generated by moving fibroblasts employed a thin polymerized film of silicone that wrinkled in response to the contractile forces exerted by moving cells via cell–substrate adhesions (Harris *et al*., 1980). Since then a variety of traction force assays have been developed, as reviewed by Beningo and Wang (2002). These include elastic nonwrinkling films of silicone (Lee *et al*., 1994; Oliver *et al*., 1998), polyacrylamide gels (Wang and Pelham, 1998), micromachined cantilevers (Galbraith and Sheetz, 1997), UV-cured wrinkling elastomers (Burton *et al*., 1999), micropatterned silicone (Balaban *et al*., 2001), gelatin substrates (Doyle and Lee, 2002), and silicone posts (Tan *et al*., 2003). Details of some of these traction force assays are the subject of other chapters in this volume. However, the basic idea behind most traction force assays is that the sensor deforms (e.g., bends in the case of cantilevers or silicone posts) in proportion to the magnitude of the traction forces exerted by motile cells. Given the material properties of an elastic substrate, such as the Young's modulus or the bending coefficient of a cantilever, it is then possible to determine the magnitude and orientation of traction stresses at discrete points beneath the cell.

An important consideration before using any traction force assay is to match the sensitivity of the sensor with the magnitude of traction forces. For example, rapidly moving cell types such as fish epidermal keratocytes are generally unable to deform polyacrylamide substrates, but can deform the more compliant silicone or gelatin. Conversely, slower moving fibroblastic cell types, which form prominent stress fibers and focal adhesions, tend to rip weakly cross-linked silicone substrates (J. Lee, unpublished observation). Since fibroblastic cells are perhaps the most common subject of cell motility studies, the majority of traction force assays have been developed for these slower moving cell types. However, it is equally important to understand mechanical events underlying the rapid movement of cells such as fish epidermal keratocytes and amoeboid cells, since they may utilize traction forces differently from fibroblastic cells.

II. Rationale

The simple shape and rapid movement of fish epidermal keratocytes make them a particularly useful model system for studying how cytoskeletal functions are organized to produce cellular movement (Lee *et al*., 1993; Svitkina *et al*., 1997). In addition, the relationship between traction force production and movement has been studied extensively in keratocytes for more than a decade (Burton *et al*., 1999; Galbraith and Sheetz, 1999; Lee *et al*., 1994; Oliver *et al*., 1998,1999). Furthermore, keratocyte movement is dependent on transient increases in intracellular calcium $[Ca^{2+}]_i$ triggered by the activation of stretch-activated calcium channels (SACs), when retraction at the rear is impeded. The ensuing calcium transient induces retraction that helps to maintain a rapid mode of movement (Lee *et al*., 1999). Thus, SAC activity may represent a critical mechanism for maintaining the high degree of coordination between protruding and retracting cell edges that is required for rapid movement. To investigate how calcium transients coordinate traction force generation in different regions of moving cells, it was necessary to develop a traction force assay that is compatible with high-resolution calcium imaging. Although nonwrinkling silicone substrates have previously been combined with calcium imaging (Lee *et al*., 1999), they were not suitable for use with traction force microscopy because changes in substrate deformation cannot be detected within the time frame of a calcium transient. This problem was compounded by the fact that the maximum substrate deformation was less than 1 μm.

Gelatin substrates possess all of the characteristics necessary to combine traction force microscopy with calcium imaging (Doyle and Lee, 2002). They are transparent and nonfluorescent (Fig. 2A). In addition, the thickness as prepared with this protocol ($\sim$40 μm) is well within the working distance of most 100$\times$ microscope objectives. An equally important feature is that gelatin substrates are highly responsive, allowing submicron bead displacements to be detected in less than 1 sec. The main limitation of gelatin substrates is that experiments must be conducted well below the melting temperature, which is typically 30 °C.

III. Methods

A. Preparation of Gelatin Substrates

The following steps produce a thin (~30 μm), highly compliant substrate, whose top surface is embedded with small (~0.2 μm) marker beads. These beads will be used for the detection of strain caused by traction forces exerted on the surface. For rapidly moving, weakly adherent cells, a gelatin concentration of 3% is recommended which has a Young's modulus of ~3 kPa. However, this concentration can be increased or decreased to make stiffer or softer gels with a Young's modulus ranging from 2.2 to 16 kPa. If the gelatin substrate is being used for the first time, we recommend that several substrates be made over a range of concentrations to determine an optimal concentration that allows both normal cell movement and detection of marker bead displacement.

1. Assemble a Rappaport chambers by attaching a glass cylinder (diameter = 22 mm, height = 8 mm) to a 22 × 22 mm^2 glass coverslip (#0 thickness), using Sylgard 184 (Dow Corning, Midland, Michigan) silicone elastomer (Fig. 1A).

2. To make a 3% gelatin gel, powdered gelatin (Nabisco, Parsippany, New Jersey) is dissolved in prewarmed (~40 °C) Ca^{2+}- and Mg^{2+}- free Fish Ringer's solution (112-mM NaCl, 2-mM D-glucose, 2-mM KCl, 2.4-mM $NaHCO_3$) for about 3 min. The gelatin solution should become clear with no observable particulates, otherwise brief vortexing should remove them.

3. Transfer a 400 μl of liquid gelatin into the Rappaport chamber and allow it to solidify in a humid environment at 4 °C for 2–24 h. Humidity is necessary to prevent gels from drying out, which will effectively increases the gelatin concentration and thus the rigidity of the substrate.

4. Dilute a solution of fluorescent microbeads (0.2-μm diameter, Molecular Probes) 1:100 in distilled water, vortex for about 1 min, then cool to 4 °C. Red or orange beads are used in conjunction with the calcium indicator (Calcium Green-1 dextran, Molecular Probes). Au2

5. Add 400 μl of the cooled bead solution to the solidified gelatin, then aspirate off immediately and leave this to dry for 1 h at 4 °C, in an environment room with good air circulation (Fig. 1B). At this time, it is useful (but not necessary) to make a small indentation with a pipette tip, at the extreme edge of the gelatin, which will serve as an indicator for the melting state of the gelatin in the next step.

6. Briefly warm the chamber with gelatin on a hot plate set at ~62 °C for 5–15 sec to liquefy only the lower layer of gelatin, then carefully aspirate ~330 μl of the solution from the bottom of the chamber using a small pipette tip, being careful not to disturb the top surface (Fig. 1C). Using the indentation as an indicator, remove the chamber from the hot plate as soon as the indentation disappears. This is a critical step, because if the gelatin liquefies completely, the marker beads will sink into it. Alternatively, if the lower layer of gelatin does not liquefy sufficiently, it will be difficult to remove a sufficient volume such that the thickness

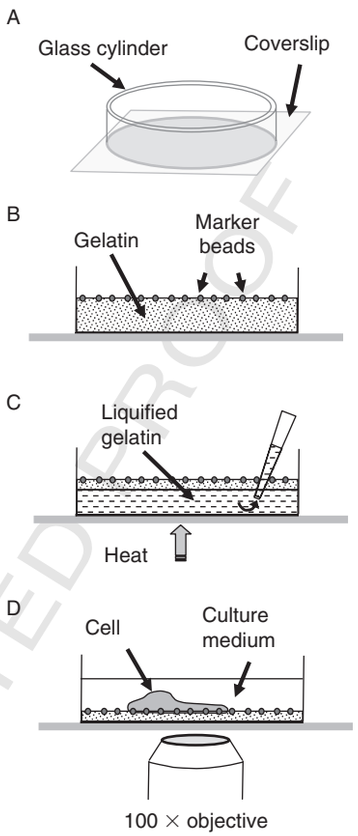

Fig. 1 Diagrams illustrating the key steps in the manufacture and use of the gelatin substrate. (A) Components of a glass Rappaport chamber. (B) Cross-section of a Rappaport chamber containing 400-μl solidified gelatin with a layer of marker beads dried on to the top surface (step 5 of the protocol). (C) Diagram showing step 6 of the protocol in which the lower layer of gelatin is heated and aspirated off. (D) The completed substrate for the traction force assay.

of the substrates falls within the working distance of the microscope objective, making it impossible to image cells on top.

7. Remove the chamber from the hot plate and rapidly cooled for 30 sec by placing on a level metal sheet, precooled to $-20\,^{\circ}C$.

8. Let the gelatin substrate sit at $4\,^{\circ}C$ for 1 h to allow complete solidification. The chamber may be stored for up to 72 h under 0.5 ml of serum-supplemented culture medium.

9. Calibrate each substrate prior to use, by measuring Young's modulus as described in another chapter of this volume, since this value will be needed for

calculation of traction stresses. This measurement should be performed after the gelatin has equilibrated to room temperature for 1 h because gelatin substrates are temperature sensitive. In addition, it is often useful to repeat these measurements after an experiment, to check for any changes in Young's modulus, especially if variations in room temperature are suspected. The elasticity gelatin substrates can be varied between ~2.2 and 16 kPa with a high degree of reproducibility by altering gelatin concentration. At gelatin concentrations of 2.5% and above and at temperatures below 26 °C, substrates behave as an ideal elastic material (Doyle and Lee, 2002). This is supported by the observation that beads during cell movement return immediately to their original undisplaced positions following release by the cell. Furthermore, when a microneedle is used to displace a single marker bead, for a distance doubling that made normally by the cell (~12 μm) and for 10 times the duration (5 min), beads return instantaneously to within ~4% (11.52 μm) of their original positions, following release.

B. Plating Cells onto a Gelatin Substrate

Some trial and error may be necessary to plate cells at a density such that there is only one cell per field of view. Otherwise if cells are too close, traction forces generated by neighboring cells will interfere. Although the following protocol has been optimized for fish epidermal keratocytes, it should be applicable to other rapidly moving cell types.

1. Bring the gelatin substrate to room temperature. Before plating cells, place ~200 μl of serum-rich culture medium, supplemented with 30% FBS, on the gelatin substrate and incubate for 30 min.

2. Epidermal sheets are obtained from explants of ~4 fish scales placed on a 22-mm^2 square coverslip within a 35-mm plastic Petri dish, as described previously (Lee *et al*., 1994). Wash explants twice with Ca^{2+}- and Mg^{2+}-free PBS (CMF-PBS) and once with a few drops of trypsin-EDTA (0.05% trypsin containing 0.53-mM EDTA, Life Technologies, Grand Island, New York). Carefully aspirate all the fluid from the Petri dish.

3. Immediately add 130 μl of a 1:1 mixture of CMF-PBS and trypsin-ETDA to the coverslip. Monitor under a microscope until cells begin to round up.

4. Immediately add 1 ml of serum-rich culture medium. Pipette the solution up and down several times (~5) to remove as many adherent cells as possible.

5. Transfer the cell-containing medium to a 1.5-ml Eppendorf tube, then *quickly* empty it onto the gelatin substrate. Note if the medium is emptied too slowly it will tend to "bead-up" on the substrate, making it difficult to spread the medium without agitating the chamber and possibly rupturing the gelatin.

6. Allow the cells to attach to the gelatin substrate for 45–60 min at room temperature before experimentation (Fig. 1D).

C. Data Collection and Analysis

The methods used for image acquisition and data analysis have been described in detail elsewhere (Doyle and Lee, 2005; Doyle *et al*., 2004), so only the key points will be covered here. Keratocyte cultures grown in plastic Petri dishes (35-mm diameter) were loaded with both the calcium indicator Calcium Green™-1 dextran (3000 MW) and a calcium insensitive, Texas red fluorescent dextran (3000 MW, Au3 Molecular Probes, Eugene, Oregon) using the Influx™ pinocytic cell-loading reagent (Molecular Probes) as previously described (Doyle *et al*., 2002) and then Au4 replated onto the gelatin substrate, embedded with blue fluorescent marker beads. Triple fluorescence imaging was performed using a Zeiss 100×/1.4 emersion oil objective on a Zeiss Axiovert 200M inverted microscope (Carl Zeiss MicroImaging, Inc., Thornwood, New York) equipped with a DG-4 filter-changer (Sutter Instruments Co., Novato, California). Three fluorescence images of Calcium Green-1, the Texas red dextran, and the marker beads were acquired using FITC, Texas Red, and Cy-5/DAPI excitation filters, respectively, every ~1.8 sec. Emitted fluorescence was collected using a DAPI/FITC/Texas Red/Cy-5 quad band-pass filter set (Chroma Technology Corp.). An Orca II CCD camera (Hamamatsu Corp., Au5 Bridgewater, New Jersey) controlled by Openlab software (Improvision) on an Au6 Apple G4 platform was used for image acquisition.

To detect changes in $[Ca^{2+}]_i$, measurements of the average fluorescence intensity were made over the cell body region in sequential, background-subtracted images. Morphometric analyses were performed using Metamorph analysis software (Universal Imaging Corp.). Cell speed was calculated using the x–y coordinates Au7 of the cell centroid. The distance between every 11th centroid was calculated (~every 20 sec), from which a running average of 5 was obtained. Cell shape was measured for each frame, in terms of a shape factor according to the following equation: shape factor $= (4\pi A)/P^2$, where A is the cell area and P is the cell perimeter. This provides a measure between 0 and 1, for how close cell shape resembles a circle, where 0 is a straight line and 1 is a circle.

A qualitative impression of the relative magnitude and direction of traction stresses can be obtained by generating a "streak" image in which pixels of maximum brightness from each image of the marker beads in a series are superimposed in a single image (Fig. 2B). This type of analysis provides a useful means for detecting: (1) any drift of marker beads, (2) the maximum bead displacement, (3) whether bead displacements are occurring outside of the field of view, and (4) the ability of all displaced beads to return to their original positions. Streak images also provide a good indication of the magnitude and direction of the traction stresses generated beneath the cell but only for cell types that maintain a simple relatively constant shape during movement such as fish keratocytes.

It is important to realize that some bead displacements may represent the response of the substrate, rather than the result of locally applied traction stresses. For example, moving keratocytes generate relatively strong "pinching" tractions at their lateral cell edges in a direction perpendicular to the direction of cell

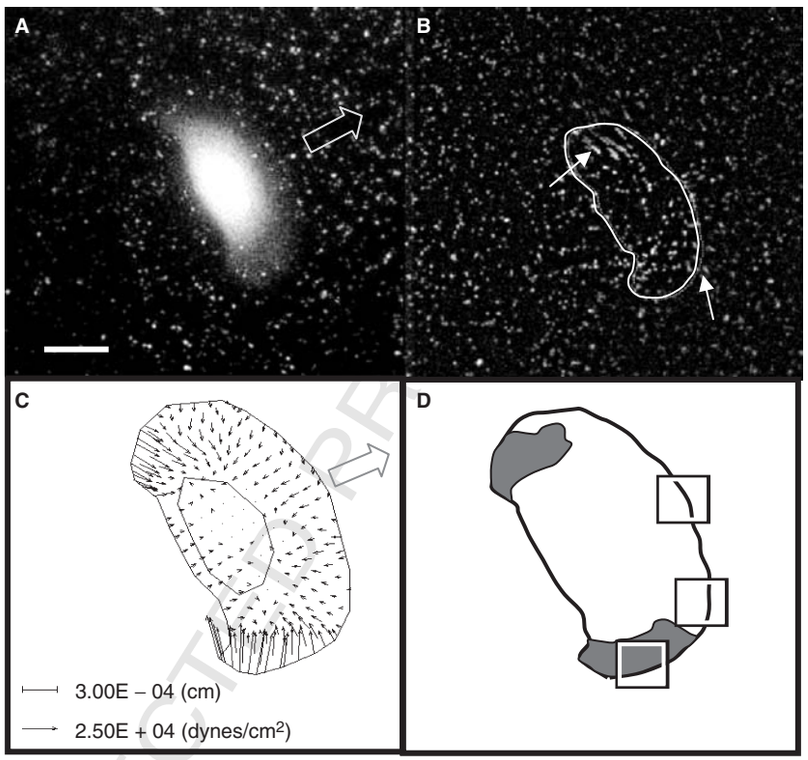

Fig. 2 Fluorescence images of the traction force assay and resulting vector and magnitude maps of traction stresses generated by a moving keratocyte. (A) Merged dual fluorescence image of a keratocyte loaded with a fluorescent calcium indicator, Calcium Green-1 dextran (excitation $\lambda = 500$ nm) moving on a gelatin substrate embedded with red fluorescent marker beads (excitation $\lambda = 560$ nm). (B) A fluorescence "streak" image showing the total bead displacements associated with a single calcium transient of 18-sec duration. Bead displacements (arrows) are clearly seen on either side of the cell (white outline) with the largest total displacements occurring on the left side. (C) A vector map generated by the LIBTRC software of traction stresses beneath a different cell. Strong tractions are oriented inward with respect to the left and right cell margins. Small inward directed tractions are also visible beneath the leading lamellipodium and at the rear cell edge. (D) A traction magnitude or "mag map" in which regions of the high traction stress, equal to or greater than the 90th percentile, are colored gray. The boxes show several sampling regions on the right side of the cell. Block arrows represent direction of cell movement. Scale bar is 10 μm.

movement that causes the substrate to be pushed outward with respect to the front and back of the cell (parallel to cell motion). To the naive observer, it may appear as if marker beads are being pushed outward by the leading cell edge. However, a given bead displacement may not accurately represent the size or direction of tractions generated by adjacent regions of the cell because the experimentally

observed pattern of bead displacements are the result of a complex integration of traction stresses generated beneath the entire ventral cell surface.

To determine the magnitude and direction of the traction stresses generated at specific locations of the ventral cell surface, we use custom software LIBTRC (Dembo and Wang, 1999; Marganski *et al*., 2003), that may be obtained from Dr. Micah Dembo. The first step is to obtain the substrate displacement field for each time point, which requires an image of beads in their displaced positions and a reference or null image of beads in their undisplaced positions, after the cell has moved away. Displacement of the substrate is calculated by comparing the positions of marker beads between the disturbed and reference image, using a correlation-based optical flow algorithm (Marganski *et al*., 2003). Using the traced cell outline as a guide, a custom algorithm is then used to generate a mesh of ~200 quadrilateral elements tessellating the interior of the cell. The most likely traction vector at each node of this mesh is then estimated by fitting the displacement data using the formulas of Boussinesque relating substrate displacement to delta function forces acting at the substrate surface (Dembo and Wang, 1999).

D. Trouble-Shooting Guide

Since gelatin substrates are made "by hand," practice is required before they are suitable for an experiment. Some common problems that are likely to be encountered by those unfamiliar with the technique are described below.

1. Marker beads are not in the same plane of focus.

This usually occurs when attempting to liquefy the lower layer of gelatin. If the Rappaport chamber is heated for a few seconds too long, the gelatin will liquefy, allowing the beads to sediment from the top surface. The most effective way to avoid this problem is to observe when the small indentation, previously made at the edge of the gelatin, disappears. If the indentation disappears too quickly, then lower the temperature of the hot plate. We usually make substrates in triplicate and choose the best ones for an experiment. These substrates should have an evenly distributed monolayer of beads at the top surface of the gelatin and none of the defects described below.

2. Marker beads are too sparse or are clumped together.

The concentration of marker beads may have to be adjusted to obtain a dense, uniform distribution (~5 beads/μm^2) since a greater number of markers allow substrate deformation to be determined with a greater resolution. Beads in solution have a tendency to clump when dried onto the gelatin. Although they can still serve as markers for deformation, the loss of spatial resolution is undesirable. To prevent bead aggregation, we sonicate the stock solution for ~10 min before use, using a cleaning sonicator (Laboratory Supplies Company, Inc., Hicksville, New York) at full power.

3. The surface of the gelatin is uneven, furrowed or cracked.

Imperfections in the surface of the gelatin usually arise during the brief period of heating and aspiration of the lower layer of liquefied gelatin. If aspiration is too rapid or the gelatin is insufficiently solated, the top surface may pucker into ripples or furrows. This can also occur if the surface of the hot plate or the precooled metal sheet (step 7 in the procedure) is not completely level. In addition, gelatin substrates will crack if they dry out, so it is important to keep them in a humid environment and/or under the culture medium. Likewise, it is important not to let the marker bead solution sit for more than 1 h while waiting for them to dry onto the gelatin surface.

4. Beads detach from the gelatin substrate.

Although not a common problem, this can occur when the gelatin begins to disintegrate, which can happen if there is more than a 5 °C rise in room temperature or if the substrate is more than ~3 days old.

5. Marker bead displacements are either undetectable or too large.

Since the magnitude of average traction stress varies among individual keratocytes, we look at several moving cells to determine whether any of them can produce detectable bead displacements. Displacements may be difficult to see in a movie sequence at a slow speed; increasing the playback speed may make small displacements more noticeable. Otherwise, the substrate may be too rigid and requires downward adjustment of gelatin concentration.

Conversely, a gelatin substrate is considered too compliant when maximal bead displacements are greater than 10 μm. This is particularly problematic if the displacements drive the beads out of focus or beyond the field of view. The gelatin concentration is adjusted in 0.5% increments until the displacements are readily detectable and the maximal bead displacements are smaller than 10 pixels.

6. Displaced beads do not return immediately to their original undisplaced positions.

Typically, this indicates that the substrate is not behaving as an elastic material and therefore should not be used in the traction force assay. Although this is usually not a problem, it is likely to occur with more compliant gelatin substrates, or when the temperature rises above 26 °C.

7. Marker beads are not in the same focal plane as the cell.

While beads on the surface may be recorded selectively by proper focusing, it is helpful to have the beads on the same focal plane as the cell particularly when using an objective of high magnification and/or high numerical aperture (NA). Sinking of beads into the substrate may be avoided by reducing the time and/or temperature for heating the gelatin, or increasing the concentration of gelatin.

8. Drift in *x*-, *y*-, or *z*-planes. Small drifts in the *x*- and *y*-directions may be corrected by software (e.g., LIBTRC per below), although it is advisable to limit any drift to no more than 10 pixels. Similarly, a small amount of focus drift can be tolerated as long as the pattern of marker beads remains recognizable by the computer program for mapping substrate deformation (Marganski *et al.*, 2003).

9. The cell stops moving.

As mentioned earlier, in most cases one can simply wait for cells to move out of the field before collecting the null-force image of marker beads. Cells that fail to move away must be removed by force. Weakly adhesive cells such as keratocytes may be removed by applying a gentle jet of culture medium through a pipette or by exposure to intense fluorescence illumination to kill the cell.

IV. Applications of the Gelatin Traction Force Assay to Study Mechanosignal Transduction in Moving Keratocytes

SACs have been shown to play an important role in regulating the movement of keratocytes (Lee *et al*., 1999). To learn more about the role of mechanochemical signaling, it is necessary to perform dual calcium and traction force microscopy. The optical and physical properties of 3% gelatin substrates are well suited for this purpose (Doyle and Lee, 2002). Changes in traction forces can be monitored during individual calcium transients over a range of ~5–30 sec (Fig. 2B). Since the methods used to perform dual calcium and traction force imaging have been described in detail elsewhere (Doyle *et al*., 2004), we will focus here on the interpretation of data obtained from this type of experiment.

To generate vector maps that reveal the distribution and magnitude of traction stresses (Fig. 2C), we use the custom traction mapping software, LIBTRC, as described by Damljanovic and Dembo in this volume (Dembo and Wang, 1999; Marganski *et al*., 2003). Additionally, to quantify the temporal relationship between SAC-induced calcium transients and traction stress, we take the value of the 90th percentile traction stress at each time point, and correlate this with the fluorescence intensity of the calcium indicator (Fig. 3B). The 90th percentile value was used because it provides a more sensitive measure of changes in traction stress than the average traction stress, which is sensitive to the spreading area of the cell, or the maximal traction stress, which may reflect outlying events.

Our results indicate that a calcium transient leads to an immediate increase in traction stress, which is maintained, despite the return of $[Ca^{2+}]_i$ to baseline, until retraction occurs. To examine the spatial distribution of traction stress, contour plots of traction stress magnitude referred to here as mag maps are generated. Ranges of traction stress magnitude are rendered in different colors (Doyle *et al*., 2004), which allow easy visualization of changes in size and distribution of traction stresses. To quantify changes in the distribution of traction stress in relation to a calcium transient, we binarize mag maps by coloring only regions of high traction stress, which we define as being equal or greater than the average 90th percentile stress for the entire series (Fig. 2D). The presence high traction stress is sampled at the front, rear, and sides of the cell within equal-sized square sampling windows (Fig. 2D). Analysis of the frequency of high traction stress appearing within the sampling window indicates that high traction stresses are present at the rearmost

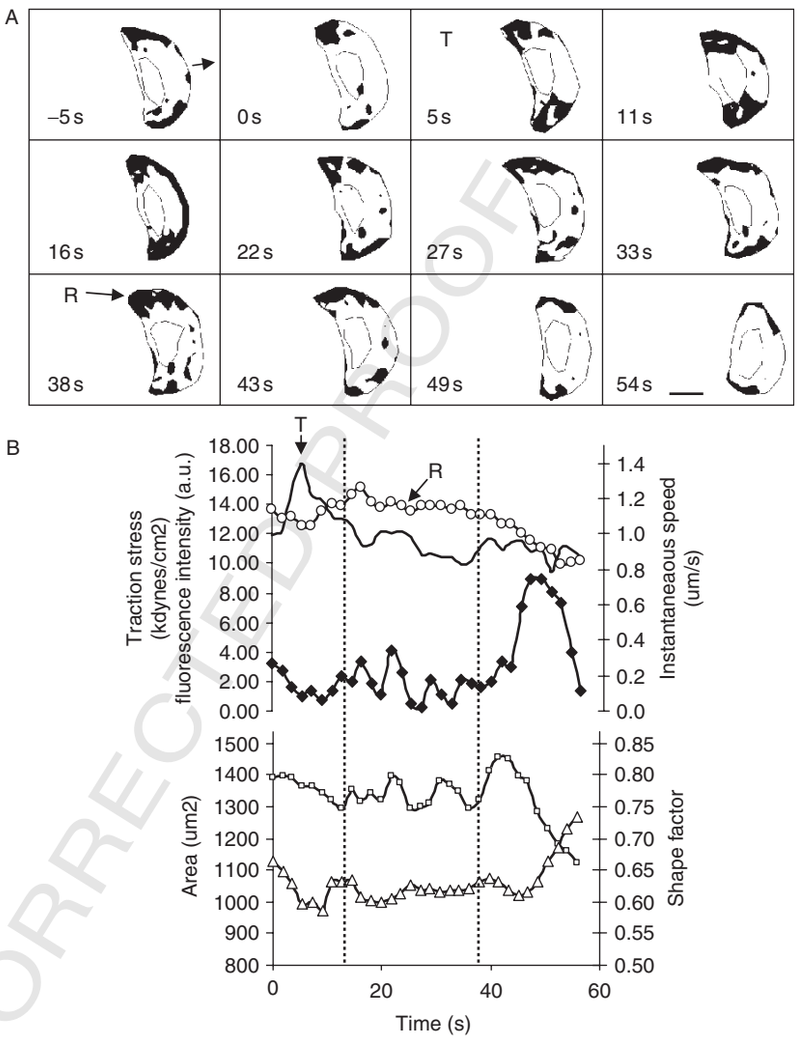

Fig. 3 Analysis of the temporal and spatial changes in high traction stress associated with a single calcium transient in a moving keratocyte. (A) Sequence of mag maps at ~5-sec intervals, corresponding to the time period in (B). The regions of high traction enlarge along the outer cell margins following a calcium transient (marked as T), then decrease on retraction (marked as R). (B) Plots of calcium indicator fluorescence (solid line), 90th percentile traction stress (line with open circles), instantaneous cell speed (solid rhomboids), cell area (open squares), and shape factor (open triangles). Decreasing values of shape factor indicate that the cell is elongating, while increasing values represent a rounding of cell shape. A single calcium transient, with a peak (T), occurs during the signal transduction phase and ends at ~13 sec (dotted line). In the following response phase, retraction (R) occurs at ~38 sec (dotted line) and ends by 54 sec.

lateral edges of the cell for the entire observation period, and for 27% and 17% of the time at the sides and front edge of the lamellipodium, respectively (Fig. 3A). The relationship between traction force generation and lamellar dynamics may be further inferred by comparing these values with the average time that the cell undergoes protrusion or retraction in each region.

To gain insight into the interrelationship between $[Ca^{2+}]_i$, traction stress, and cell movement, we compare the plot of 90th percentile traction stress with changes in cell speed, shape, and area during a single calcium transient (Doyle and Lee, 2005; Fig. 3B). The following events occur with a high degree of consistency among keratocytes. Prior to a calcium increase, which we term the ''sensing'' phase, a decrease in cell speed usually accompanies an increase in cell elongation, indicating that cell movement is inhibited by the failure to retract (data not shown). During the subsequent ''transduction'' phase, a calcium transient is followed immediately by a rise in traction stress. However, cell speed remains reduced and the cell is still elongated indicating that movement is still impeded. In addition, the degree of cell elongation at this stage suggests that cytoskeletal tension is being maintained. During the ''response phase,'' retraction is marked by a drop in traction stress and an increase in speed, as cytoskeletal tension is released and the cell resumes movement.

V. Other Applications and Future Directions

Cells that exhibit rapid amoeboid movement, such as *Dictyostelium discoideum*, leukocytes, and highly metastatic transformed cells, typically generate weaker traction forces compared with slow moving cells such as fibroblasts, which have been measured in the majority of past traction force studies. The gelatin substrate is sufficiently sensitive to detect the weak traction stress ($\sim 7 \times 10^2$ Pa) of wild-type (WT) *D. discoideum* and even myosin II null mutants that generate tractions an order of magnitude lower (Lombardi *et al*., unpublished data). Furthermore, the existence of many cytoskeletal mutants makes *Dictyostelium* a particularly useful model system to investigate the mechanism of traction mechanics. Studying the spatiotemporal patterns of traction stress in various mutants of *Dictyostelium* should provide insight into the role of different cytoskeletal components in generating and coordinating traction forces. In addition, gelatin substrate has enabled the study of GFP-myosin II redistribution in relation to traction force production in moving *Dictyostelium* (Lombardi *et al*., unpublished data). Similar studies may be applied to other fast moving cell types such as leukocytes, metastatic cells, and neurons during pathfinding. However, if cells need to be maintained at 37 °C, preparation of gelatin substrates can be modified to increase their thermal stability (Bigi *et al*., 2001).

The transparency of gelatin substrates permits its use in combination with a variety of fluorescence and photomanipulation techniques. Cells expressing fluorescent proteins or biosensors may be used to allow simultaneous observations of

the dynamics of molecular machinery and generation of traction forces. Measurements of traction forces may be further combined with fluorescence resonance energy transfer (FRET), fluorescence recovery after photobleaching (FRAP), photoactivation, and chromophore-assisted laser inactivation (CALI) to allow real-time observation and manipulation of protein activities in relation to traction force generation. The highly elastic nature of gelatin substrates will be particularly advantageous for detecting small, rapid changes in traction stress in relation to localized molecular events.

VI. Summary

The use of gelatin substrates to study traction forces generated by rapidly moving cells represents an important addition to the repertoire of assays currently available to investigate the mechanics of cell motility. The major advantage of gelatin substrate is that it is sensitive enough to detect changes in the spatiotemporal pattern of traction stresses over short timescales, for example, during individual SAC-induced calcium transients.

In addition to the preparation of gelatin substrate and its application to keratocytes, we show how to extract information from a time series of traction maps and how to interpret these data in relation to the mechanochemical regulation of keratocyte movement. We further discuss future applications of this assay, including its use in conjunction with fluorescence imaging and photomanipulation techniques and applications to other rapidly moving cell types. Together these approaches will play an important role in furthering our understanding of cellular mechanosensing.

Acknowledgments

The work described herein was supported by a National Science Foundation grant MCB-0114231 to J.L.

References

Balaban, N. Q., Schwarz, U. S., Riveline, D., Goichberg, P., Tzur, G., Sabanay, I., Mahalu, D., Safran, S., Bershadsky, A., Addadi, L., and Geiger, B. (2001). Force and focal adhesion assembly: A close relationship studied using elastic micropatterned substrates. *Nat. Cell Biol.* **3,** 466–472. Au9

Beningo, K. A., and Wang, Y.-L. (2002). Flexible substrates for the detection of cellular traction forces. *Trends Cell Biol.* **12,** 79–84.

Bigi, A., Cojazzi, G., Panzavolta, S., Rubini, K., and Roveri, N. (2001). Mechanical and thermal properties of gelatin films at different degrees of glutaraldehyde crosslinking. *Biomaterials* **22,** 763–768.

Burton, K., Park, J. H., and Taylor, D. L. (1999). Keratocytes generate traction forces in two phases. *Mol. Biol. Cell* **10**(11), 3745–3769.

Chen, C. S., Mrksich, M., Huang, S., Whitesides, G. M., and Ingber, D. E. (1997). Geometric control of cell life and death. *Science* **276**(5317), 1425–1428.

Chicurel, M. E., Chen, C. S., and Ingber, D. E. (1998). Cellular control lies in the balance of forces. *Curr. Opin. Cell Biol.* **10,** 232–239.

Dembo, M., and Wang, Y.-L. (1999). Stresses at the cell-to-substrate interface during locomotion of fibroblasts. *Biophys. J.* **76,** 2307–2316.

Doyle, A. D., and Lee, J. (2002). Simultaneous, real-time imaging of intracellular calcium and traction force production. *Biotechniques* **22**(2), 358.

Doyle, A., and Lee, J. (2005). Cyclic changes in keratocyte speed and traction stress arise from the Ca^{2+}-dependent regulation of cell adhesiveness. *J. Cell Sci.* **118**(Pt. 2), 369–379.

Doyle, A., Marganski, W., and Lee, J. (2004). Calcium transients induce spatially coordinated increases in traction force during the movement of fish keratocytes. *J. Cell Sci.* **117**(Pt. 11), 2203–2214.

Dunn, G. A., and Brown, A. F. (1986). Alignment of fibroblasts on grooved surfaces described by a simple geometric transformation. *J. Cell Sci.* **83,** 313–340.

Galbraith, C. G., and Sheetz, M. P. (1997). A micromachined device provides a new bend on fibroblast traction forces. *Proc. Natl. Acad. Sci. USA* **94**(17), 9114–9118. Au11

Galbraith, C. G., and Sheetz, M. P. (1999). Keratocytes pull with similar forces on their dorsal and ventral surfaces. *J. Cell Biol.* **147**(6), 1313–1323. Au12

Harris, A. K., Wild, P., and Stopak, D. (1980). Silicone rubber substrates: A new wrinkle in the study of cell locomotion. *Science* **208**(4440), 177–179.

Janmey, P. A. (1998). The cytoskeleton and cell signaling: Component localization and mechanical coupling. *Physiol. Rev.* **78,** 763–781.

Lauffenburger, D. A., and Horwitz, A. F. (1996). Cell migration: A physically integrated molecular process. *Cell* **84**(3), 359–369.

Lee, J., Ishihara, A., Oxford, G., Johnson, B., and Jacobson, K. (1999). Regulation of cell movement is mediated by stretch-activated calcium channels. *Nature* **400,** 382–386.

Lee, J., Ishihara, A., Theriot, J. A., and Jacobson, K. (1993). Principles of locomotion for simple-shaped cells. *Nature* **362,** 167–171.

Lee, J., Leonard, M., Oliver, T., Ishihara, A., and Jacobson, K. (1994). Traction forces generated by locomoting keratocytes. *J. Cell Biol.* **127,** 1957–1964.

Lo, C., Wang, H. B., Dembo, M., and Wang, Y. L. (2000). Cell movement is guided by the rigidity of the substrate. *Biophys. J.* **79,** 144–152.

Malek, A. M., and Izumo, S. (1996). Mechanism of edothelial shape change and cytoskeletal remodeling in response to fluid shear stress. *J. Cell Sci.* **109,** 713–726.

Marganski, W. A., Dembo, M., and Wang, Y.-L. (2003). Measurements of cell-generated deformations on flexible substrates using correlation-based optical flow. *Methods Enzymol.* **161,** 197–211.

Oliver, T., Dembo, M., and Jacobson, K. (1999). Separation of propulsive and adhesive traction stresses in locomoting keratocytes. *J. Cell Biol.* **145**(3), 589–604.

Oliver, T., Jacobson, K., and Dembo, M. (1998). Design and use of substrates to measure traction forces exerted by cultured cells. *Methods Enzymol.* **298,** 497–488.

Pender, N., and McCullouch, C. A. G. (1991). Quantitation of actin polymerization in two human fibroblast sub-types responding to mechanical stretching. *J. Cell Sci.* **100,** 187–193.

Schwarzbauer, J. E. (1997). Cell migration: May the force be with you. *Curr. Biol.* **7,** R292–R294.

Sheetz, M. P., Felsenfeld, D. P., and Galbraith, C. (1998). Cell migration: Regulation of force on extracellular-matrix-integrin complexes. *Trends Cell Biol.* **8,** 51–54.

Svitkina, T. M., Verkhovsky, A. B., McQuade, K. M., and Borisy, G. (1997). Analysis of the actin-myosin II system in fish epidermal keratocytes: Mechanism of cell body translocation. *J. Cell Biol.* **139**(2), 397–415.

Tan, J. L., Tien, J., Pirone, D. M., Gray, D. S., Bhadriraju, K., and Chen, C. S. (2003). Cells lying on a bed of microneedles: An approach to isolate mechanical force. *Proc. Natl. Acad. Sci. USA* **100,** 1484–1489.

Wang, N., and Ingber, D. E. (1994). Control of cytoskeletal mechanics by extracellular matrix, cell shape, and mechanical tension. *Biophys. J.* **66,** 2181–2189.

Wang, Y.-L., and Pelham, R. J. (1998). Preparation of a flexible porous polyacrylamide substrate for mechanical studies of cultured cells. *Methods Enzymol.* **298,** 489–496.

Further Reading

Dembo, M., Oliver, T., Ishihara, A., and Jacobson, K. (1996). Imaging the traction stresses exerted by locomoting cells with the elastic substrate method. *Biophys. J.* **70,** 2008–2022. Au10

Italiano, J. E., Stewart, M., and Roberts, T. M. (2001). How the assembly dynamics of the nematode major sperm protein generate amoeboid cell motility. *Int. Rev. Cytol.* **2002,** 1–34. Au13

Li, Y., Hu, Z., and Li, C. (1993). New method for measuring Poisson's ratio in polymer gels. *J. Appl. Polym. Sci.* **50,** 1107–1111. Au14

Wang, N., Ostuni, E. O., Whitesides, G. M., and Ingber, D. E. (2002). Micropatterning tractional forces in living cells. *Cell Motil. Cytoskeleton* **52,** 97–106. Au8

Author Query

Methods in Cell Biology, 83
Article No.: Chapter 12

ELSEVIER

Dear Author,

During the preparation of your manuscript for typesetting some questions have arisen. These are listed below. Please check your typeset proof carefully and mark any corrections in the margin of the proof or compile them as a separate list. This form should then be returned with your marked proof/list of corrections to Elsevier Science.

Disk use

In some instances we may be unable to process the electronic file of your article and/or artwork. In that case we have, for efficiency reasons, proceeded by using the hard copy of your manuscript. If this is the case the reasons are indicated below:

☐ Disk damaged ☐ Incompatible file format ☐ LaTeX file for non-LaTeX journal

☐ Virus infected ☐ Discrepancies between electronic file and (peer-reviewed, therefore definitive) hard copy.

☐ Other: .....

We have proceeded as follows:

☐ Manuscript scanned ☐ Manuscript keyed in ☐ Artwork scanned

☐ Files only partly used (parts processed differently:.....)

Bibliography

If discrepancies were noted between the literature list and the text references, the following may apply:

☐ The references listed below were noted in the text but appear to be missing from your literature list. Please complete the list or remove the references from the text.

☐ Uncited references: This section comprises references which occur in the reference list but not in the body of the text. Please position each reference in the text or, alternatively, delete it. Any reference not dealt with will be retained in this section.

Query Refs.	Details Required
Author	**Further Reading section:** Some of your references may appear in a "Further Reading" section at the end of the chapter. These are references that were found to be uncited in the text, and have been called out to your attention. This is only temporary. To ensure that the called out references appear in the reference list, please cite them in the appropriate spot within the text. We appreciate your cooperation.

Query Refs.	Details Required	Author's response
AU1	Please check the change.	
AU2	Please provide manufacturer's location (in case of USA, state only).	
AU3	Please provide unit if necessary.	
AU4	This reference is not provided in the reference list. Please provide complete bibliographic details.	

AU5	Please provide manufacturer's location (in case of USA, state only).	
AU6	Please provide location if this is a manufacturer (in case of USA, state only).	
AU7	Please provide manufacturer's location (in case of USA, state only).	
AU8	This reference is not cited in text. Please provide citation within the text.	
AU9	As per style et al. is only used in the reference after 12 author names. Please check the insertion of author name (in all such cases).	
AU10	This reference is not cited in text. Please provide citation within the text.	
AU11	Please check the deletion of "a" and insertion of initials for accuracy.	
AU12	Please check the insertion of initial names for accuracy.	
AU13	This reference is not cited in text. Please provide citation within the text.	
AU14	This reference is not cited in text. Please provide citation within the text.	

Typesetter Query

Attention authors: Please address every typesetter query below. Failure to do so may result in references being deleted from your proofs. Thanks for your cooperation.

Query Refs.	Details Required	Author's response
1.	Please provide correct page range for the reference ''Oliver *et al.*, 1998.''	